DOI: 10.1002/ejic.200801082

Synthesis, Crystal Structure, and Thermal and Magnetic Properties of New Transition Metal–Pyrazine Coordination Polymers

Mario Wriedt,[a] Inke Jeß,[a] and Christian Näther*[a]

Keywords: N ligands / Coordination polymers / Crystal structures / Thermal properties / Magnetic properties

The reaction of nickel thiocyanate with pyrazine in a 1:2 ratio leads to the new ligand-rich 1:2 (ratio metal/ligand) compound $[Ni(SCN)_2(pyrazine)_2]_n$ (**1**), in which the metal atoms are coordinated by four N atoms of pyrazine ligands and two N atoms of thiocyanate anions in a slightly distorted octahedral arrangement. If an excess of the metal thiocyanate is used and the reaction is performed under solvothermal conditions, single crystals of the ligand-deficient 1:1 compounds $[M(SCN)_2(pyrazine)_2]_n$ [M = Fe (**2I**), Co (**3**), Ni (**4**)] are obtained. Compound **2I** is isotypic with $[Mn(SCN)_2(pyrazine)]_n$ but different to **3** and **4**, which are also isotypic. Investigations on the synthesis of these compounds reveal that only compound **4** can be prepared phase-pure in solution; all other ligand-deficient compounds are always contaminated with large amounts of the corresponding ligand-rich coordination polymers. In the crystal structures, the metal atoms are surrounded by two N atoms of the pyrazine ligands as well as by two N atoms and two S atoms of the thiocyanate anions in a slightly distorted octahedral geometry. In contrast to the ligand-rich 1:2 coordination polymers, the metal atoms are further linked into layers by the thiocyanate anions due to μ_2-*N*,*S* coordination. On heating, compound **1** and the ligand-rich 1:2 coordination polymers $[M(SCN)_2(pyrazine)_2]_n$ (M = Fe, Co) transform quantitatively into the ligand-deficient compounds. Surprisingly, thermal decomposition of the iron compound leads to a new modification (**2II**), which is isotypic to compounds **3** and **4**. The magnetic properties of all compounds have been investigated and are found to be dependent on the connection mode of the thiocyanate anions.

Introduction

We have recently reported thermal decomposition reactions for the preparation of new ligand-deficient coordination compounds from copper(I), silver(I), zinc(II), or cadmium(II) halides,[1] all of which are diamagnetic transition metals, and N-donor ligands. In further work we investigated whether this method can also be used for the preparation of coordination polymers based on paramagnetic transition metals and reported a coordination polymer based on manganese thiocyanate and pyrazine.[2] Only one compound of composition $[Mn(SCN_2)(pyrazine)_2]_n$ has been reported to date and its magnetic behavior investigated.[3] The crystal structure of the more ligand-rich 1:4 compound $[M(SCN_2)(pyrazine)_4]$ was also reported a few years later.[4] The Mn^{2+} cations in the ligand-rich compound $[Mn(SCN_2)(pyrazine)_2]_n$ are coordinated by four N atoms of pyrazine ligands and two N atoms of thiocyanate anions in a slightly distorted octahedral environment. The Mn^{2+} ions are further connected into layers by the pyrazine ligands due to μ-*N*,*N*′ coordination, and the thiocyanate anions do not act as bridging ligands. On heating, the ligand-rich 1:2 compound loses half of its pyrazine ligands to form the ligand-deficient 1:1 compound $[Mn(SCN_2)(pyrazine)]_n$, in which the Mn cations are linked by the thiocyanate anions into chains, which are further connected into layers by the N-donor ligands. Magnetic measurements have revealed that the ligand-rich 1:2 compound exhibits only weak antiferromagnetic interactions, whereas the latter shows antiferromagnetic ordering, which is obviously mediated by the thiocyanate anions, at about 26 K.

The crystal structures and magnetic properties of the ligand-rich 1:2 compounds with iron and cobalt have also been investigated.[3,5–8] Interestingly, however, the corresponding ligand-deficient compounds were not reported. This might be due to the fact that these compounds cannot be prepared in solution, although they are easily accessible by thermal decomposition of their ligand-rich 1:2 precursor compounds.

In this work we report on the structural, thermal and magnetic properties of new and recently discovered transition metal–pyrazine compounds with Fe, Co, and Ni.

[a] Institut für Anorganische Chemie, Universität zu Kiel, Max-Eyth-Straße 2, 24098 Kiel, Germany
Fax: +49-431-880-1520
E-mail: cnaether@ac.uni-kiel.de
Supporting information for this article is available on the WWW under http://www.eurjic.org or from the author.

Results and Discussion

Crystal Structures

The ligand-rich 1:2 compound $[Ni(SCN)_2(pyrazine)_2]_n$ (**1**) crystallizes in the centrosymmetric monoclinic space group *C*2/*m* with two formula units in the unit cell and is isotypic with the ligand-rich 1:2 manganese,[3] iron,[5] and cobalt[9] compounds reported recently. The asymmetric unit consists of one Ni^{2+} cation, which occupies the position 2/*m*, one thiocyanate anion, which is located on a crystallographic mirror plane, and one pyrazine ligand, which is located on a center of inversion. The Ni^{2+} cations in the crystal structure are coordinated by four pyrazine ligands and two thiocyanate anions in a slightly distorted octahedral arrangement (Figure 1, top). The thiocyanate anions do not act as bridging ligands and are only coordinated to the metal center through the N atom. The Ni–N distances to the negatively charged nitrogen atom of the thiocyanate anion are significantly shorter than those to the nitrogen atom of the N-donor ligand (Table 1). The Ni^{2+} ions are connected by the pyrazine ligands by μ-*N*,*N*′ coordination to form layers, which are perpendicular to the crystallographic *c* axis (Figure 1, bottom).

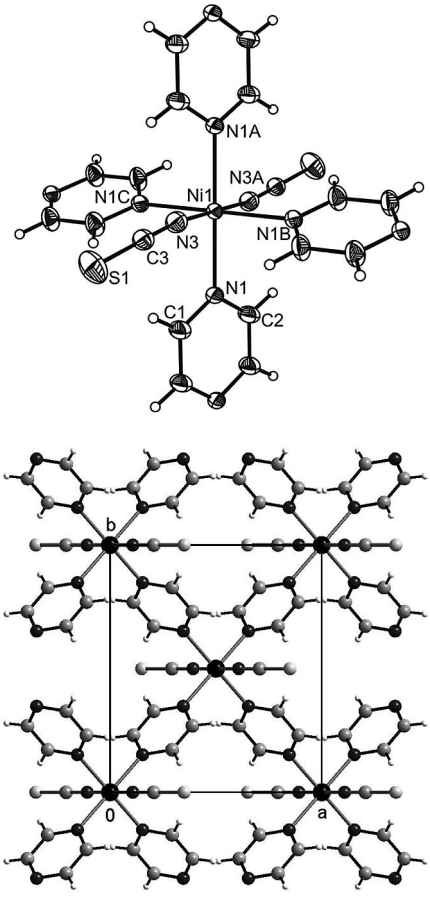

Figure 1. Crystal structure of the 1:2 nickel compound **1** showing the coordination sphere of the nickel cations with labeling and displacement ellipsoids drawn at the 50% probability level (top) and the layers of the structure in the direction of the crystallographic *c* axis (bottom). Symmetry codes: A: –*x*, –*y*, –*z* + 1; B: –*x*, *y*, –*z* + 1; C: *x*, –*y*, *z*.

Table 1. Selected bond lengths [Å] and angles [°] for the 1:2 nickel compound **1**.

Ni(1)–N(1)	2.1622(13)	N(3)–Ni(1)–N(1A)	90.34(6)
Ni(1)–N(3)	2.033(2)	N(1)–Ni(1)–N(1C)	91.73(7)
S(1)–C(3)	1.624(3)	N(3A)–Ni(1)–N(3)	180.0
C(3)–N(3)	1.163(4)	N(1A)–Ni(1)–N(1)	180.0
N(1A)–Ni(1)–N(1C)	88.27(7)	N(1C)–Ni(1)–N(1B)	180.00(8)
N(3)–Ni(1)–N(1)	89.66(6)		

The ligand-deficient 1:1 compounds $[M(SCN)_2(pyrazine)]_n$ [M = Fe (**2I**), Co (**3**), Ni (**4**)] crystallize in the centrosymmetric monoclinic space group *C*2/*m* with two formula units in the unit cell. The iron compound **2I** is isotypic with the manganese compound.[2] Compounds **3** and **4** are also isotypic but crystallize with different cell parameters to compound **2I** (Table 6). Each asymmetric unit consists of one M^{2+} cation and one pyrazine ligand, which occupies the position 2/*m*, as well as one thiocyanate anion located on a crystallographic mirror plane. The pyrazine ligand in compounds **3** and **4** is disordered in two orientations due to symmetry. A similar disorder is also observed in space groups *C*2 or *Cm*, and there is no evidence of super-structure reflections. The crystal of compound **4** investigated was nonmerohedrally twinned. Both individuals were indexed and integrated separately and the overlapping reflections were omitted.

The M^{2+} cations are coordinated by two pyrazine ligands and two S and two N atoms of four symmetry-related thiocyanate anions in a slightly distorted octahedral geometry (Figure 2). In contrast to the ligand-rich compound **1**, the metal cations are each connected by two thiocyanate anions in a μ_2-*N*,*S* coordination mode to form chains along the *c* axis. These chains are connected by the pyrazine ligands into layers (Figure 3). A comparison of the 1:1 compounds shows an explicit trend of shortening M–NCS, M–SCN, and $M–N_{pyrazine}$ distances upon going from manganese to nickel as well as a small change in the NCS–M–NCS angles and the intra- and intermolecular metal–metal distances, in good agreement with the ionic radii (Mn^{2+} 0.97, Fe^{2+} 0.92, Co^{2+} 0.90, and Ni^{2+} 0.84 Å)[10] (see Tables 2 and 3).

Synthetic Aspects

The formation and stability of the compounds was investigated in solution by solvent-mediated conversion experiments, whereby an excess of metal salt and N-donor ligand are mixed in different stoichiometric ratios (1:6, 1:5, 1:4, 1:3, 1:2, 2:3, 1:1, 2:3, 2:1, 3:1, 4:1) in water. All reactions led to a precipitate, which was stirred for 3 d in order to obtain the thermodynamically most stable compounds. The products were then investigated by X-ray powder diffraction. These experiments clearly showed that the ligand-rich 1:2 compounds $[M(SCN)_2(pyrazine)_2]_n$ [M = Fe,[5] Co[9] and Ni (**1**)] are formed for practically all stoichiometries except for the ligand-deficient 1:1 nickel compound **4**, which can

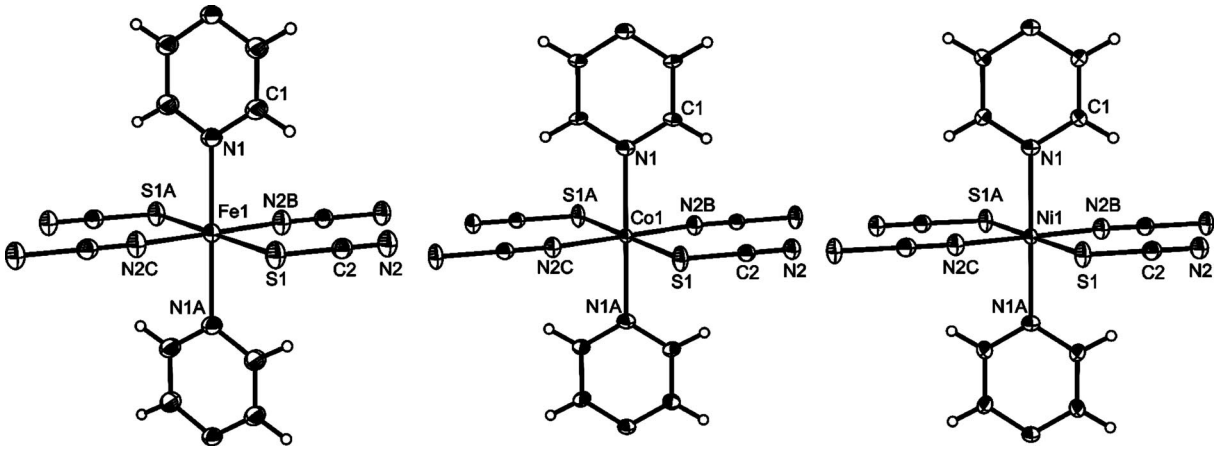

Figure 2. Crystal structures of the 1:1 iron **2I** (left), cobalt **3** (middle), and nickel **4** (right) compounds, showing the coordination sphere of the metal cations and atom labeling. Displacement ellipsoids are drawn at the 50% probability level. Disorder is not shown for clarity. Symmetry codes: A: $-x, -y + 1, z$; B: $-x, -y + 1, -z + 1$; C: $x, y, z + 1$ for **2I**; A: $-x + 1, -y + 1, -z + 2$; B: $x, y, z - 1$; C: $-x + 1, -y + 1, -z + 1$ for **3**; A: $-x, -y, -z$; B: $x, y, z - 1$; C: $-x, -y, -z + 1$ for **4**.

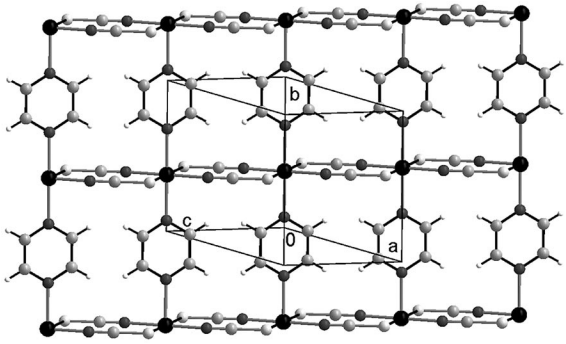

Figure 3. Crystal structures of the ligand-deficient 1:1 compounds $[M(SCN)_2(pyrazine)]_n$ [M = Fe (**2I**), Co (**3**), Ni (**4**)] showing the layers. Disorder has been omitted for clarity.

Table 2. Comparison of selected bond lengths [Å] and angles [°] for the ligand-deficient 1:1 Mn,[2] Fe (**2I**), Co (**3**), and Ni (**4**) compounds.

1:1 compound	Mn[2]	Fe (**2I**)	Co (**3**)	Ni (**4**)
M(1)–N(1)	2.327(2)	2.257(3)	2.183(3)	2.129(3)
M(1)–N(2B)	2.126(2)	2.073(3)	2.063(3)	2.031(3)
M(1)–S(1)	2.7071(8)	2.6377(9)	2.5746(10)	2.5215(9)
S(1)–C(2)	1.639(3)	1.642(3)	1.642(4)	1.645(4)
C(3)–N(2)	1.159(4)	1.165(5)	1.157(5)	1.160(5)
N(2C)–M(1)–S(1)	87.58(7)	87.49(9)	86.67(9)	86.31(9)
N(2B)–M(1)–S(1)	92.42(7)	92.51(9)	93.33(9)	93.69(9)
N(1)–M(1)–S(1)	90.0	90.0	90.0	90.0
N(2B)–M(1)–N(1)	90.0	90.0	90.0	90.0
N(2B)–M(1)–N(1A)	90.0	90.0	90.0	90.0
N(2B)–M(1)–N(2C)	180.0	180.0	180.0	180.0
S(1)–M(1)–S(1A)	180.0	180.0	180.0	180.0
N(1A)–M(1)–N(1)	180.00(10)	180.0	180.0	180.00(18)
N(2)–C(2)–S(1)	179.8(3)	178.9(3)	180.0(3)	180.00(5)

be prepared phase-pure with a 4:1 excess of metal salt in solution. A small amount of single crystals of the ligand-deficient 1:1 compounds was obtained as the minor phase in a mixture with the ligand-rich 1:2 compounds under hydrothermal conditions, although they could never be obtained phase-pure in solution. Thus, we investigated whether the ligand-deficient compounds could be prepared by a thermal decomposition reaction.

Table 3. Comparison of the intra- and intermolecular metal–metal distances [Å] for the ligand-deficient 1:1 Mn,[2] Fe (**2I**), Co (**3**), and Ni (**4**) compounds.

1:1 compound	Mn[2]	Fe (**2I**)	Co (**3**)	Ni (**4**)
M–SCN–M (intra)	5.765	5.696	5.663	5.609
M–pyrazine–M (intra)	7.455	7.622	7.161	7.056
M–M (inter)	6.486	6.413	6.755	6.733

Thermoanalytical Investigations (DTA-TG-MS)

On heating of the ligand-rich 1:2 compounds $[M(SCN)_2(pyrazine)_2]_n$ [M = Fe,[5] Co[9] and Ni (**1**)] in a thermobalance to 500 °C, two well-resolved mass-loss steps were observed in the TG curve, which are accompanied by endothermic events in the DTA curve. TG measurements of the 1:2 cobalt compound have been reported by Lu et al.,[9] although the intermediate products were not characterized. The MS trend scan curve shows that only the N-donor ligand (m/z = 80) is lost during these steps (Figure 4). The experimental mass losses of the first two events are in good agreement with those calculated for a stepwise removal of the pyrazine ligand (Table 4). The DTG curve shows that both events are well separated (Figure 4).

Based on the observed mass losses, it can be confirmed that the ligand-deficient 1:1 compounds $[M(SCN)_2(pyrazine)]_n$ [M = Fe (**2I**), Co (**3**), Ni (**4**)] are formed in the first step. On further heating, the remaining ligands are lost to give $M(SCN)_2$, which decomposes on further heating (Figure 4).

In order to verify the nature of the intermediates formed, additional TG measurements with heating rates of 4 °C/min were performed and stopped after the first TG step. An investigation of the residues by elemental analysis (see Ex-

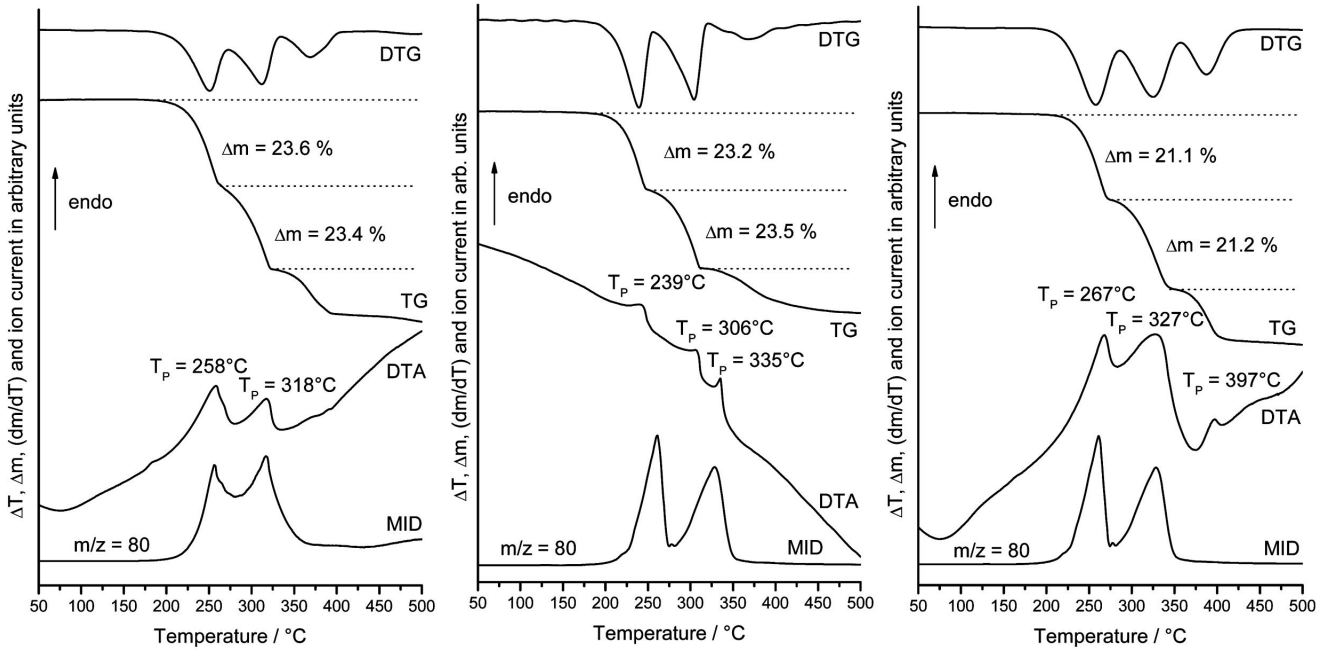

Figure 4. DTA, TG, DTG, and MS trend scan curves for the ligand-rich 1:2 compounds $[Fe(SCN)_2(pyrazine)_2]_n$[5] (left), $[Co(SCN)_2(pyrazine)_2]_n$[9] (middle), and $[Ni(SCN)_2(pyrazine)_2]_n$ (**1**; right). Heating rate: 4 °C/min; *m/z* = 80 [pyrazine]. The mass changes [%] and the peak temperatures T_P [°C] are given.

Table 4. Comparison of the experimental mass losses with the calculated mass losses for the loss of 1 mol of pyrazine from the ligand-rich 1:2 compounds.

1:2 compound	Fe[5]	Co[9]	Ni (**1**)
Δ*m* for first step	23.6	23.2	21.1
Δ*m* for second step	23.4	23.5	21.2
Δ*m* calculated (–1 mol pyrazine)	24.1	23.9	23.9

perimental Section) and X-ray powder diffraction showed that the ligand-deficient 1:1 compounds had been formed very pure (Figure 5). Interestingly, the ligand-deficient 1:1 iron compound obtained by thermal decomposition is isotypic with compounds **3** and **4** (cf. Figure 5A with Figure 5C and E). Thus, a new polymorphic modification **2II** has been formed. It should be noted, however, that compound **2II** is always contaminated with very small amounts of compound **2I** (see arrows in Figure 5A).

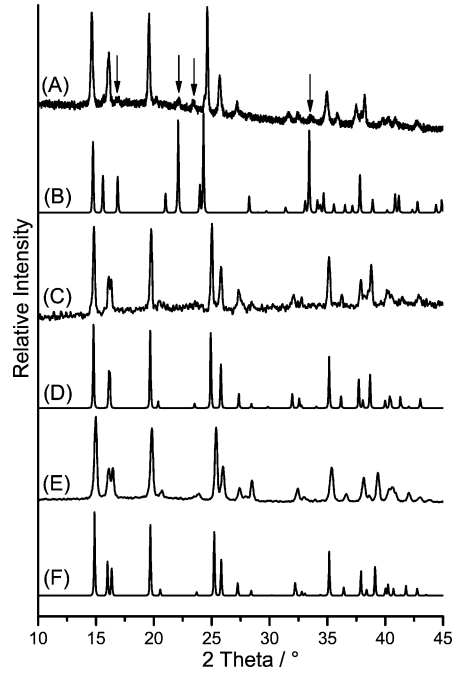

Figure 5. Experimental XPRD patterns for the residue obtained after the first TG step in the thermal decomposition reaction of the ligand-rich 1:2 compounds $[Fe(SCN)_2(pyrazine)_2]_n$[5] (A), $[Co(SCN)_2(pyrazine)_2]_n$[9] (C), and $[Ni(SCN)_2(pyrazine)_2]_n$ (**1**; E) and calculated XPRD patterns for the ligand-deficient 1:1 compounds $[Fe(SCN)_2(pyrazine)]_n$ (**2I**; B), $[Co(SCN)_2(pyrazine)]_n$ (**3**; D), and $[Ni(SCN)_2(pyrazine)]_n$ (**4**; F). The arrows indicate the position of the reflections of compound **2I**.

Magnetic Investigations

Cooperative magnetic phenomena arising from the connection of the metal centers through the small-sized thiocyanate ligands might be expected for the ligand-deficient 1:1 iron (**2II**), cobalt (**3**), and nickel (**4**) compounds, as has been reported previously for $[Mn(SCN)_2(pyrazine)]_n$.[2] Magnetic measurements were therefore performed for all ligand-rich 1:2 and ligand-deficient 1:1 compounds. It should be noted that form **2II** was investigated for the ligand-deficient 1:1 iron compound, because form **2I** cannot be prepared phase-pure in solution and is always obtained as the minor phase in a mixture with the ligand-rich 1:2 compound. Form **2II** prepared by thermal decomposition always contains a very small amount of form **2I**, but this was neglected, because the composition and the topology of the coordination network remains constant.

The magnetic susceptibilities were measured as a function of temperature in the range 2–300 K at B_0 = 1 T (Figure 6). The data were corrected for diamagnetic contributions by using an increment of -50×10^{-6} emu mol^{-1} for the pyrazine ligand, -13×10^{-6} emu mol^{-1} for Fe^{2+}, -12×10^{-6} emu mol^{-1} for Co^{2+} and Ni^{2+} and -31×10^{-6} emu mol^{-1} for the thiocyanate anion.[11] The ligand-rich 1:2 iron, cobalt, and nickel compounds were measured some decades

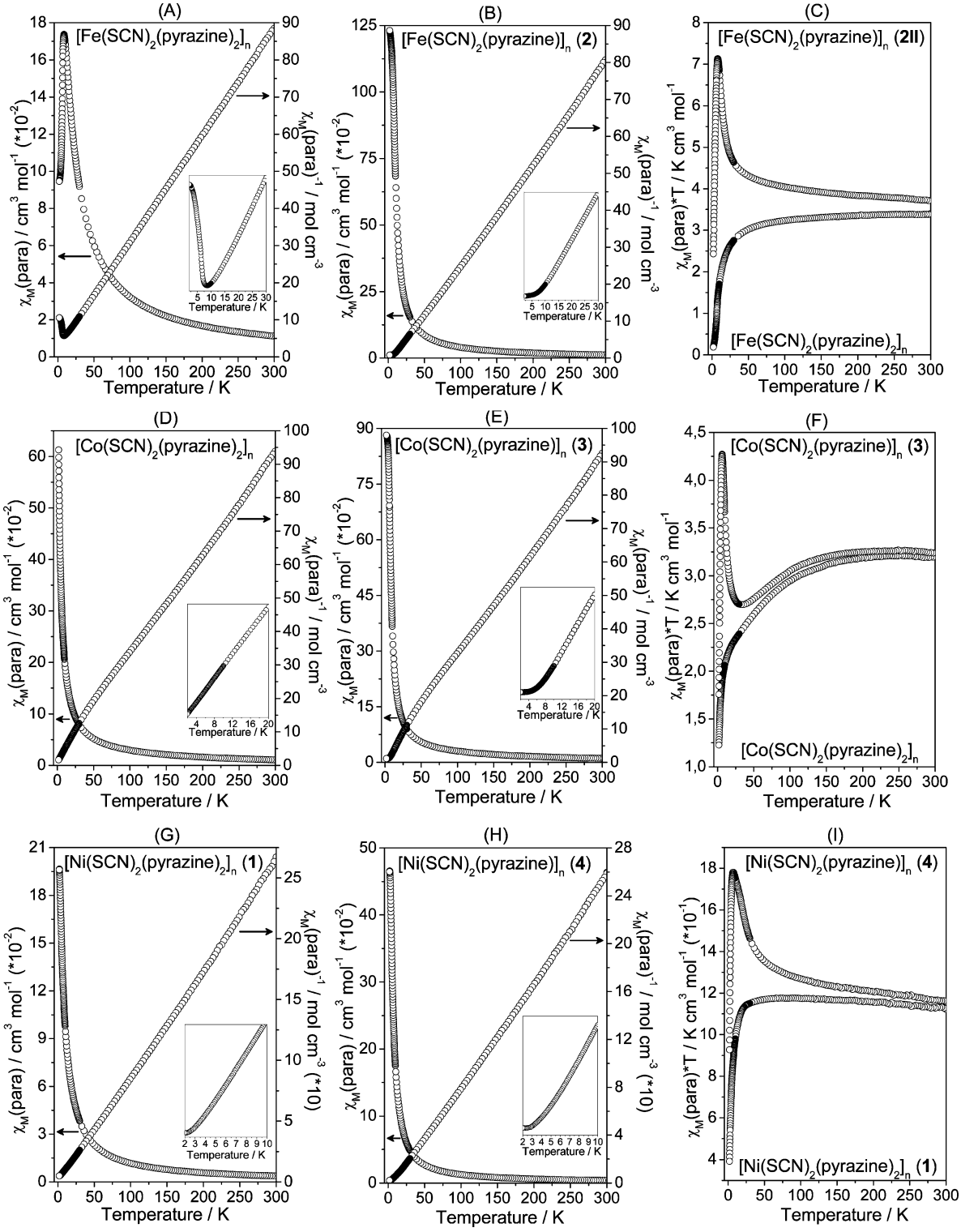

Figure 6. Paramagnetic susceptibility (left side in graphs A, B, D, E, G, H), reciprocal paramagnetic susceptibility (right side in graphs A, B, D, E, G, H), and $\chi_M T$ (graphs C, F, I) as a function of temperature for the ligand-rich 1:2 and ligand-deficient 1:1 iron (top), cobalt (middle), and nickel (bottom) compounds. The insets in graphs A, B, D, E, G and H show the variation of the Curie–Weiss law at lower temperatures.

Table 5. Results according to the Curie–Weiss law for the ligand-rich 1:2 and ligand-deficient 1:1 compounds.

	1:2 compound				1:1 compound			
	Mn[2,3]	Fe[3,5,6,7]	Co[3,8]	Ni[3] (**1**)	Mn[2]	Fe (**2II**)	Co (**3**)	Ni (**4**)
C [cm^3 K mol^{-1}]	4.51	3.48	3.38	1.13	4.36	3.64	3.37	1.14
θ [K]	–1.72	–7.80	–14.15	2.03	–69.55	9.60	–9.12	9.04
μ_{eff} (exp) [μ_B]	6.00	5.28	5.20	3.01	5.90	5.39	5.20	3.02
μ_{eff} (calc)[10] [μ_B]	5.92	4.90	3.87	2.83	5.92	4.90	3.87	2.83
T_N [K]	–	8.51	–	–	26.00	–	–	–
Fit [K]	10–300	20–300	50–300	20–300	60–300	30–300	80–300	25–300

ago by Real et al.,[5] Haynes et al.,[6] Figgis et al.,[7] and Lloret et al.,[3,8] but for a more accurate comparison with the ligand-deficient 1:1 compounds they were remeasured in our laboratory to lower temperatures. Figure 6 displays the results of the susceptibility measurements in the form of χ_M vs. T, χ_M^{-1} vs. T and $\chi_M T$ vs. T plots, and Table 5 presents the results obtained upon fitting the data to the Curie–Weiss law $\chi_M = C/(T - \theta)$.

For the ligand-rich 1:2 iron compound, a sharp maximum is observed in the χ_M vs. T curve, which indicates an antiferromagnetic ordering at T_N = 8.5 K mediated by the pyrazine ligand (Figure 6A). The negative Weiss constant (θ = –7.8 K; Table 5) and the decrease of the $\chi_M T$ vs. T curve upon cooling confirms this antiferromagnetic behavior (Figure 6C). In contrast, only Curie–Weiss paramagnetism is found for the ligand-deficient 1:1 iron compound **2II**. The χ_M^{-1} vs. T curve is essentially linear (Figure 6B), and the positive Weiss constant (θ = 9.6 K; Table 5) indicates ferromagnetic interactions between the Fe^{2+} metal sites joined through the μ_2-*N*,*S* thiocyanato anions. The $\chi_M T$ vs. T curve increases gradually upon cooling to around 50 K due to ferromagnetic interactions. Below this temperature, $\chi_M T$ increases to a maximum value of 7.1 K cm^3 mol^{-1} at 8 K due to rapidly increasing ferromagnetic correlations between adjacent spin carriers. Upon cooling to 2 K, $\chi_M T$ decreases quickly (Figure 6C). A similar magnetic behavior has been reported by Manson et al.[12] for $[Mn(N_3)_2(pyrazine)]_n$, which exhibits the same topology for the coordination network, and was interpreted as interchain antiferromagnetic interactions through the bridging pyrazine ligands.

The χ_M^{-1} vs. T curve for the ligand-rich 1:2 cobalt compound is linear, which is characteristic of pure paramagnetic behavior (Figure 6D). The negative Weiss constant (θ = –14.2 K; Table 5) indicates antiferromagnetic interactions between the Co^{2+} centers, which lead to a decrease of the $\chi_M T$ values upon cooling (Figure 6F). Compared to the latter compound, the ligand-deficient 1:1 cobalt compound **3** shows paramagnetic behavior down to around 10 K (Figure 6E). The decrease in the $\chi_M T$ values upon cooling to around 36 K and the negative Weiss constant (θ = –9.1 K; Table 5) indicate antiferromagnetic interactions between the Co^{2+} centers (Figure 6F). Below this temperature, $\chi_M T$ increases to a maximum value at 6 K, as observed for the 1:2 iron compound (see above).

The magnetic behaviors of the ligand-rich 1:2 nickel compound **1** (Figure 6G) and the ligand-deficient 1:1 nickel compound **4** (Figure 6H) are almost the same as for the cobalt compounds, except the slight increases in the $\chi_M T$ values (Figure 6I) upon cooling to 66 K and the positive Weiss constant (θ = 2.0 K; Table 5) for **1**, and the increase in the $\chi_M T$ values (Figure 6I) to a maximum at 7 K and the positive Weiss constant (θ = 9.0 K; Table 5) for **4**, which indicate weak ferromagnetic interactions between the Ni^{2+} centers.

It is difficult to explain why only the ligand-deficient 1:1 manganese compound[2] shows an antiferromagnetic ordering at lower temperatures, whereas the corresponding Fe (**2II**), Co (**3**), and Ni (**4**) compounds do not, especially as the topologically identical ligand-deficient 1:1 cobalt compound $[Co(SCN)_2$(dimethylpyrazine *N*,*N*′-dioxide)$]_n$ also shows antiferromagnetic behavior.[13] The bond lengths and angles as well as the intra- and intermolecular metal–metal distances of the ligand-deficient compounds $[M(SCN)_2$(pyrazine)$]_n$ (M = Mn, Fe, Co, Ni) are almost the same (Tables 2 and 3), therefore structural differences can be excluded. It is also surprising that the ligand-rich 1:2 iron compound shows an antiferromagnetic ordering at lower temperatures, which is not observed in the ligand-rich 1:2 manganese, cobalt, and nickel compounds.

Conclusion

We have presented four new coordination compounds based on metal thiocyanates and pyrazine ligands and have shown that thermal decomposition reactions are an alternative tool for discovering additional ligand-deficient phases. One of the advantages of this method is that decomposition reactions of suitable precursor compounds must lead to components with a higher degree of condensation. If the precursors are based on paramagnetic transition metals and small-sized ligands, the preparation of compounds with interesting magnetic properties is possible. However, the magnetic phenomena are sometimes difficult to understand, because compounds with identical coordination network topologies sometimes show completely different magnetic behaviors. Much more systematic investigations are needed for a better understanding, therefore similar coordination polymers based on small-sized ligands like thiocyanates, cyanates, and formates with N-donor ligands like pyrazine, pyrimidine, and 4,4′-bipyridine will be investigated in the future. We confidently expect to synthesize a large number of new compounds with interesting magnetic behavior during such investigations.

Experimental Section

Synthesis: All compounds were prepared by stirring the reactants in water at room temperature for 3 d. The residues were filtered off and washed with ethanol and diethyl ether and dried in air. The purity of these compounds was checked by X-ray powder diffraction and elemental analysis.

$[Ni(SCN)_2(pyrazine)_2]_n$ (1): A blue crystalline powder was isolated from the reaction between $NiCl_2{\cdot}6H_2O$ (237.7 mg, 1.0 mmol), KSCN (194.4 mg, 2.0 mmol), and pyrazine (160.2 mg, 2.0 mmol) in water (5.0 mL). Yield: 292.6 mg (88.1%). $C_{10}H_8N_6NiS_2$ (335.04): calcd. C 35.85, H 2.41, N 25.08, S 19.14; found C 35.63, H 2.26, N 24.73, S 19.33. IR (KBr): $\tilde{\nu}$ = 3441 (m), 3123 (w), 3060 (w), 2083 (s), 1629 (w), 1491 (w), 1416 (m), 1165 (m), 1126 (m), 1058 (m), 974 (w), 803 (m), 476 (m) cm^{-1}. Blue single crystals were isolated by heating $Ni(SCN)_2$ (43.7 mg, 0.25 mmol) with pyrazine (40.1 mg, 0.5 mmol) in water (3 mL) in a closed test tube at120 °C for 1 d.

$[Fe(SCN)_2(pyrazine)]_n$ (2I): Orange-brown single crystals were isolated from the reaction between $FeSO_4{\cdot}7H_2O$ (139.0 mg, 0.5 mmol), KSCN (97.2 mg, 1.0 mmol), and pyrazine (10.0 mg, 0.125 mmol) in water (3.0 mL) in a closed test tube at 120 °C after 4 d. The product consisted of single crystals of compound **2I** as the minor phase and the ligand-rich 1:2 compound as the major phase.

$[Co(SCN)_2(pyrazine)]_n$ (3): Orange single crystals were isolated from the reaction between $Co(SCN)_2{\cdot}xH_2O$ (48.3 mg, 0.25 mmol) and pyrazine (5.0 mg, 0.0625 mmol) in ethanol (0.4 mL) in a closed test tube at 120 °C after 5 d. The product consists of single crystals of compound **3** as the minor phase and the ligand-rich 1:2 compound as the major phase.

$[Ni(SCN)_2(pyrazine)]_n$ (4): A green crystalline powder was isolated from the reaction between $Ni(SCN)_2$ (699.4 mg, 4.0 mmol) and pyrazine (80.1 mg, 1.0 mmol) in water (5.0 mL) after one week. Yield: 247.8 mg (97.2%). $C_6H_4N_4NiS_2$ (254.95): calcd. C 28.27, H 1.58, N 21.98, S 25.16; found C 28.47, H 1.53, N 21.51, S 24.68. IR (KBr): $\tilde{\nu}$ = 3461 (m), 3094 (w), 2123 (s), 1632 (w), 1490 (w), 1419 (m), 1166 (w), 1124 (w), 1059 (m), 806 (m), 479 (m) cm^{-1}. Green single crystals were isolated from the reaction between $Ni(SCN)_2$ (43.7 mg, 0.25 mmol) and pyrazine (5 mg, 0.0625 mmol) in methanol (3 mL) in a closed test tube at 120 °C after 5 d.

$[Fe(SCN)_2(pyrazine)_2]_n$: An orange crystalline powder was isolated from the reaction between $FeSO_4{\cdot}7H_2O$ (278.0 mg, 1.0 mmol), KSCN (194.4 mg, 2.0 mmol), and pyrazine (160.2 mg, 2.0 mmol) in water (5.0 mL). Yield: 292.6 mg (88.1%). $C_{10}H_8FeN_6S_2$ (332.19): calcd. C 36.16, H 2.43, N 25.30, S 19.31; found C 35.82, H 2.33, N 24.89, S 20.02. IR (KBr): $\tilde{\nu}$ = 3449 (m), 3132 (w), 3048 (w), 2359 (w), 2056 (s), 1636 (w), 1486 (w), 1416 (m), 1161 (w), 1112 (w), 1052 (m), 798 (w), 456 (m) cm^{-1}.

$[Co(SCN)_2(pyrazine)_2]_n$: A pink crystalline powder was isolated from the reaction between $CoCl_2{\cdot}6H_2O$ (237.9 mg, 1.0 mmol), KSCN (194.4 mg, 2.0 mmol), and pyrazine (160.2 mg, 2.0 mmol) in water (5.0 mL). Yield: 289.1 mg (86.2%). $C_{10}H_8CoN_6S_2$ (335.28): calcd. C 35.82, H 2.41, N 25.07, S 19.13; found C 35.53, H 2.33, N 24.92, S 19.18. IR (KBr): $\tilde{\nu}$ = 3444 (m), 3118 (w), 3053 (w), 2065 (s), 1633 (w), 1490 (w), 1415 (m), 1163 (m), 1127 (m), 1055 (m), 969 (w), 800 (m), 465 (m) cm^{-1}.

Elemental Analysis of the Residues Obtained in the Thermal Decomposition: (A) Calculated (for 1:1 iron compound **2II**): C 28.59, H 1.60, N 22.22, S 25.44; found (for compound isolated after first heating step for 1:2 iron compound) C 28.39, H 1.54, N 22.48, 25.54. (B) Calculated (for 1:1 cobalt compound **3**): C 28.24, H 1.58, N 21.95, S 25.13; found (for compound isolated after first heating step for 1:2 cobalt compound) C 28.06, H 1.52, N 22.08, S 25.26. (C). Calculated (for 1:1 nickel compound **4**): C 28.27, H 1.58, N 21.98, S 25.16; found (for compound isolated after first heating step for 1:2 nickel compound **1**) C 28.47, H 1.53, N 21.57, S 24.92.

Single-Crystal Structure Analysis: All investigations were performed with an imaging plate diffraction system (IPDS-1) with Mo-K_α radiation from STOE & CIE. The structures were solved

Table 6. Selected crystal data and details on the structure determinations.

Compound	**1**	**2I**	**3**	**4**
Empirical formula	$C_{10}H_8N_6NiS_2$	$C_6H_4FeN_4S_2$	$C_6H_4CoN_4S_2$	$C_6H_4N_4NiS_2$
M/L ratio	1:2	1:1	1:1	1:1
Formula mass [g mol^{-1}]	335.05	252.10	255.18	254.96
Crystal system	monoclinic	monoclinic	monoclinic	monoclinic
Space group	*C*2/*m*	*C*2/*m*	*C*2/*m*	*C*2/*m*
a [Å]	9.9283(16)	10.5311(11)	11.4570(18)	11.4697(12)
b [Å]	10.2127(19)	7.3224(10)	7.1608(8)	7.0560(6)
c [Å]	7.2079(12)	5.6957(6)	5.6630(9)	5.6086(5)
β [°]	118.498(10)	94.588(12)	104.892(18)	105.127(11)
V [Å^3]	642.29(19)	437.80(9)	448.99(11)	438.18(7)
T [K]	293	293	293	293
Z	2	2	2	2
$D_{calcd.}$ [g cm^{-3}]	1.732	1.912	1.888	1.932
μ [mm]$^{-1}$	1.828	2.149	2.327	2.640
Min/max transmission	–/–	0.6955/0.7670	0.6706/0.7435	–/–
θ_{max} [°]	60.05	56.18	55.84	55.96
Measured reflections	2165	1973	2153	2468
Unique reflections	991	573	576	436
Reflections [$F_o > 4\sigma(F_o)$]	835	484	493	396
Parameters	51	38	47	47
R_{int}	0.0477	0.0322	0.0711	0.0435
R_1[a] [$F_o > 4\sigma(F_o)$]	0.0277	0.0325	0.0338	0.0296
wR_2[b] (all data)	0.0733	0.0869	0.0806	0.0780
GOF	1.003	1.008	1.013	1.058
Residual electron density [e Å^{-3}]	0.445/–0.466	0.403/–0.438	0.366/–0.538	0.412/–0.454

[a] $R_1 = \Sigma||F_o| - |F_c||/\Sigma|F_o|$. [b] $wR_2 = \{\Sigma[w(F_o^2 - F_c^2)^2]/\Sigma[w(F_o^2)^2]\}^{1/2}$.

by direct methods using SHELXS-97,[14] and structure refinements were performed against F^2 by using SHELXL-97.[15] A numerical absorption correction was applied by using X-Red[16] and X-Shape[17] for compounds **2I** and **3**. All non-hydrogen atoms were refined with anisotropic displacement parameters. All hydrogen atoms were positioned with idealized geometries and were refined with fixed isotropic displacement parameters [U_{eq}(H) = –1.2 U_{eq}(C)] for aromatic H atoms by using a riding model with $d_{C–H}$ = 0.98 Å. Details of the structure determination are given in Table 6. CCDC-713059 (**1**), -713060 (**2I**), -713061 (**3**) and -713062 (**4**) contain the supplementary crystallographic data for this paper. These data can be obtained free of charge from the Cambridge Crystallographic Data Center via www.ccdc.cam.uk/data_request.cif.

X-ray Powder Diffraction (PXRD): PXRD experiments were performed by using a STOE DF4 transmission powder diffractometer with Cu-K_α radiation (λ = 154.0598 pm) equipped with a position-sensitive detector (scan range: 5–45°) from STOE & CIE.

Differential Thermal Analysis, Thermogravimetry, and Mass Spectrometry (DTA-TG-MS): The DTA-TG measurements were performed under nitrogen (purity: 5.0) in Al_2O_3 crucibles with an STA-409CD instrument from Netzsch. The DTA-TG-MS measurements were performed with the same instrument connected to a quadrupole mass spectrometer from Balzers through a Skimmer coupling from Netzsch. The MS measurements were performed in analogue and trend scan mode in Al_2O_3 crucibles under dynamic helium (purity: 5.0) by using heating rates of 4 °C/min. All measurements were performed with a flow rate of 75 mL/min and were corrected for buoyancy and current effects. The instrument was calibrated by using standard reference materials.

Elemental Analysis: C,H,N analyses were performed with an EURO EA elemental analyzer manufactured by EURO VECTOR Instruments and Software.

Spectroscopy: FT IR spectra were recorded with a Genesis series FTIR spectrometer, by ATI Mattson, in KBr pellets.

Supporting Information (see footnote on the first page of this article): Experimental and calculated X-ray powder patterns for the ligand rich compounds as well as IR spectra of all compounds.

Acknowledgments

M. W. thanks the Stiftung Stipendien-Fonds des Verbandes der Chemischen Industrie and the Studienstiftung des deutschen Volkes for a PhD scholarship. Moreover, we gratefully acknowledge financial support by the State of Schleswig-Holstein and the Deutsche Forschungsgemeinschaft (project NA 720/1-1). We thank Professor Dr. Wolfgang Bensch for allowing us to use his experimental facilities.

[1] a) G. Bhosekar, I. Jeß, N. Lehnert, C. Näther, *Eur. J. Inorg. Chem.* **2008**, 605–611; b) G. Bhosekar, I. Jess, C. Näther, *Inorg. Chem.* **2006**, *45*, 6508–6515; c) I. Jeß, C. Näther, *Z. Naturforsch., Teil B* **2007**, *62*, 617–620; d) I. Jeß, C. Näther, *Inorg. Chem.* **2006**, *45*, 7446–7454; e) C. Näther, A. Beck, *Z. Naturforsch., Teil B* **2004**, *59*, 992–998; f) C. Näther, G. Bhosekar, I. Jeß, *Eur. J. Inorg. Chem.* **2007**, 5353–5359; g) C. Näther, J. Greve, I. Jeß, *Solid State Sci.* **2002**, *4*, 813–820; h) C. Näther, I. Jeß, *J. Solid State Chem.* **2002**, *169*, 103–112; i) C. Näther, I. Jeß, *Z. Naturforsch., Teil B* **2002**, *57*, 1133–1140; j) C. Näther, I. Jess, *Inorg. Chem.* **2003**, *42*, 2968–2976; k) C. Näther, I. Jeß, J. Greve, *Polyhedron* **2001**, *20*, 1017–1022; l) C. Näther, I. Jeß, N. Lehnert, D. Hinz-Hübner, *Solid State Sci.* **2003**, *5*, 1343–1357; m) C. Näther, I. Jeß, H. Studzinski, *Z. Naturforsch., Teil B* **2001**, *56*, 997–1002.
[2] C. Näther, J. Greve, *J. Solid State Chem.* **2003**, *176*, 259–265.
[3] F. Lloret, M. Julve, J. Cano, G. D. Munno, *Mol. Cryst. Liq. Cryst.* **1999**, *334*, 569–585.
[4] T. Liu, Z.-P. Xie, *Acta Crystallogr., Sect. E* **2007**, *63*, m1820–m1820.
[5] J. A. Real, G. D. Munno, M. C. Munoz, M. Julve, *Inorg. Chem.* **1991**, *30*, 2701–2704.
[6] J. S. Haynes, A. Kostikas, J. R. Sams, A. Simopoulos, R. C. Thompson, *Inorg. Chem.* **1987**, *26*, 2630–2637.
[7] B. N. Figgis, J. Lewis, F. E. Mabbs, G. A. Webb, *J. Chem. Soc. A* **1967**, 442–447.
[8] F. Lloret, G. D. Munno, M. Julve, J. Cano, R. Ruiz, A. Caneschi, *Angew. Chem. Int. Ed.* **1998**, *37*, 135–138.
[9] J. Lu, T. Paliwala, S. C. Lim, C. Yu, T. Niu, A. J. Jacobson, *Inorg. Chem.* **1997**, *36*, 923–929.
[10] A. F. Holleman, E. Wiberg, *Lehrbuch der Anorganischen Chemie*, 101st ed., de Gruyter, Berlin, New York, **1995**.
[11] G. A. Bain, J. F. Berry, *J. Chem. Educ.* **2008**, *85*, 532–536.
[12] J. L. Manson, A. M. Arif, J. S. Miller, *Chem. Commun.* **1999**, 1479–1480.
[13] J.-M. Shi, Y.-M. Sun, X. Zhang, L. Yi, P. Cheng, L.-D. Liu, *J. Phys. Chem. A* **2006**, *110*, 1677–7681.
[14] G. M. Sheldrick, *SHELXS-97, Program for Crystal Structure Solution*, University of Göttingen, Germany, **1997**.
[15] G. M. Sheldrick, *SHELXL-97, Program for the Refinement of Crystal Structures*, University of Göttingen, Germany, **1997**.
[16] *X-Red, Program for Data Reduction and Absorption Correction*, STOE & CIE GmbH, Darmstadt, Germany, **1998**, version 1.11.
[17] *X-Shape, Program for the Crystal Optimization for Numerical Absorption Correction*, STOE & CIE GmbH, Darmstadt, Germany, **1998**, version 1.03.

Received: November 5, 2008
Published Online: February 26, 2009

